Low-intensity low-frequency ultrasound enhances the chemosensitivity of gemcitabine-resistant ASPC-1 cells via PI3K/AKT/NF-κB pathway-mediated ABC transporters

FUQIANG QIU, JIFAN CHEN, JING CAO, FENG DIAO and PINTONG HUANG

Department of Ultrasound, The Second Affiliated Hospital of Zhejiang University School of Medicine, Hangzhou, Zhejiang 310000, P.R. China

Received December 1, 2019; Accepted June 23, 2020

DOI: 10.3892/or.2020.7671

Abstract. Tumor drug resistance (TDR) invariably leads to the failure of chemotherapy. In addition, current treatment strategies for TDR are not satisfactory due to limitations in terms of safety and feasibility. The aim of the present study was to determine whether low-intensity low-frequency ultrasound (LILFU) could improve the effect of chemotherapy and reverse TDR in gemcitabine-resistant ASPC-1 (ASPC-1/GEM) cells. The investigation focused on the association between LILFU effectiveness and the adenosine triphosphate-binding cassette (ABC) transporters and the phosphoinositide 3-kinase (PI3K)/protein kinase B (AKT)/nuclear factor (NF)-κB signaling pathway. A Cell Counting Kit-8 assay was used to determine the appropriate acoustic intensity, half-maximal inhibitory concentration of gemcitabine (GEM) and the viability of ASPC-1/GEM cells. ASPC-1/GEM cells were divided into control, GEM, LILFU and GEM+LILFU groups. Cell proliferation was evaluated through colony formation assays, whereas cell apoptosis was detected using flow cytometry. Western blotting was used to explore the expression levels of ABC transporters and PI3K/AKT/NF-κB signaling pathway-associated proteins. Xenograft models in mice were established to identify the enhancing effect of GEM+LILFU *in vivo*. Immunohistochemistry was used to detect the expression levels of Ki-67 in tumor tissues. The acoustic parameter of 0.2 W/cm^2 and a GEM concentration of 6.63 mg/ml were used in subsequent experiments. Following treatment with GEM+LILFU, the cell viability and proliferation ability were decreased, whereas the apoptotic rate was increased compared with the GEM group. The expression levels of ABC transporters, *PI3K-P110α* and *NF-κB* were decreased in the GEM+LILFU group. Notably, LILFU increased the effectiveness of GEM in inhibiting tumor growth, and reduced the expression levels of Ki-67 in the xenograft mouse model. LILFU improved the chemosensitivity of ASPC-1/GEM cells via inhibition of cell viability and proliferation, and promoted cell apoptosis in the GEM+LILFU group. In conclusion, LILFU may downregulate the expression levels of ABC transporters by inhibiting the PI3K-p110α/AKT/NF-κB signaling pathway, thereby reversing resistance in pancreatic cancer.

Correspondence to: Professor Pintong Huang, Department of Ultrasound, The Second Affiliated Hospital of Zhejiang University School of Medicine, 88 Jiefang Road, Jianggan, Hangzhou, Zhejiang 310000, P.R. China
E-mail: huangpintong@zju.edu.cn

Key words: shockwave therapy, tumor drug resistance, pancreatic cancer, gemcitabine, PI3K/AKT/NF-κB pathway, adenosine triphosphate-binding cassette transporters

Introduction

Pancreatic ductal adenocarcinoma (PDAC) is exceptionally malignant, progressive and typically associated with poor prognosis, with a 5-year survival rate of only 5-15% (1). In 2018, 55,000 patients with pancreatic cancer were newly diagnosed in the United States, and 44,330 patients died. It is reasonable to estimate that, by 2030, pancreatic cancer will be the second leading cause of cancer-associated mortality (2-4).

Gemcitabine (GEM) is well established as a standard drug for patients with PDAC, improving the survival rate of patients and bringing marked therapeutic benefits since its discovery several decades ago (5). However, only 20-30% of patients with PDAC benefit from GEM treatment, and its therapeutic effect is limited despite co-administration with other chemotherapeutic agents. The unfavorable outcome is largely attributed to the development of tumor drug resistance (TDR) (6-8).

TDR is one of the bottlenecks in tumor therapy, and various mechanisms involved in TDR have been described (9,10). One of the well-established mechanisms involves the adenosine triphosphate-binding cassette (ABC) transporters, which are membrane transporter proteins that decrease the endocellular accumulation of a drug using the energy produced from the decomposition of adenosine triphosphate (11-14). At present, 15 ABC transporters have been demonstrated to serve a role as drug pumps in TDR. Specifically, P glycoprotein (P-gp), ABC subfamily G member 2 (ABCG2) and multidrug resistance-associated protein 1 (MRP1) are positively associated with TDR in PDAC (15). Although numerous studies have reported on inhibitors of ABC transporters to overcome TDR,

their side effects and suboptimal safety profile limit the application of these agents (16-18). Furthermore, previous studies have demonstrated that the activation of the phosphoinositide 3-kinase (PI3K)/protein kinase B (AKT) signaling pathway is associated with a decreased drug effect in human breast adenocarcinoma and hepatocellular carcinoma (19-21). Therefore, inhibitors of PI3K or AKT in combination with chemotherapeutic drugs have a synergistic effect in cancer therapy (22,23). Nuclear factor (NF)-κB is vital for the development of drug resistance by regulating the expression levels of numerous genes (24). A previous study revealed that 3,3'-diindolylmethane could inhibit the activation of NF-κB, resulting in the chemosensitization of tumors (25,26). However, inhibitors of PI3K/AKT/NF-κB invariably lead to unacceptable side effects.

Low-intensity low-frequency ultrasound (LILFU) is a physical stimulus that can open cell membranes, and increase the transmission of molecules and genes via the sonoporation effect. Recently, LILFU has been recognized as a safe and effective method in tumor therapy, offering high penetrating ability and the advantage of contact with deep organs compared with other non-invasive techniques, such as light beam treatment. As physical energy, LILFU can be applied to relatively limited areas. Therefore, it has the advantage of accuracy, low systemic toxicity and few side effects. Nevertheless, few studies have focused on the efficacy and feasibility of this method to increase chemosensitivity *in vivo*, and the underlying mechanism of the enhancing effect of LILFU.

The present study aimed to demonstrate whether LILFU could enhance the cytotoxicity and therapeutic effect of GEM in GEM-resistant ASPC-1 cells both *in vitro* and *in vivo*, and to illustrate the role of ABC transporters and the PI3K/AKT/NF-κB signaling pathway in the LILFU-induced reversal of TDR.

Materials and methods

Cell culture. ASPC-1/GEM cells (American Type Culture Collection) were cultured in Roswell Park Memorial Institute (RPMI)-1640 medium (HyClone; Cytiva) supplemented with 10% fetal bovine serum (Biological Industries), penicillin G (100 U/ml) and streptomycin (100 g/ml; Sigma-Aldrich; Merck KGaA) in an incubator at 37˚C with 5% carbon dioxide. The medium was supplemented with GEM (1 μg/ml; Hanson Pharma) to maintain the drug-resistant phenotype. The cells were cultured in drug-free medium for 1 week prior to the experiments.

Exposure to LILFU. An ultrasound probe with an HPCTB-360 transducer (China Shipbuilding Industry Corporation 715 Research Institute) was used for ultrasound stimulation. The transducer used degassed sterile water in the device, and was settled on steel supports to maintain a distance of 20 mm between the transducer and the cells in the 6-well plates. The parameters of the ultrasound were as follows: 360 kHz, 50% duty cycle (on 3 sec, off 3 sec), 1 min.

Determination of the optimal LILFU parameters and the half-maximal inhibitory concentration of GEM. ASPC-1/GEM cells ($1x10^6$ cells/well) were seeded in 6-well plates and exposed to LILFU with different acoustic intensities (0, 0.06, 0.20, 0.40, 0.67 and 1.10 W/cm^2) to determine the optimal acoustic intensity of LILFU. Following incubation for 24 h, cell viability was detected using a Cell Counting Kit-8 (CCK-8) assay (Dojindo Molecular Technologies, Inc.). Furthermore, $1x10^6$ cells/well were seeded in 6-well plates and incubated with different concentrations of GEM (0, 0.625, 1.25, 2.5, 5.0 and 10 mg/ml). After 24 h of treatment, cell viability was detected using the CCK-8 assay.

Cell cytotoxicity assay. ASPC-1/GEM cells were treated with LILFU, GEM or GEM+LILFU for 24 h and seeded into 96-well plates (1,000 cells/well). Furthermore, ASPC-1/GEM cells were treated with GEM, GEM+A66 (Beyotime Institute of Biotechnology), GEM+TGX221 (Beyotime Institute of Biotechnology) or GEM+BAY11-7082 (Beyotime Institute of Biotechnology) for 24 h and seeded into 96-well plates (1,000 cells/well). A66, TGX221 and BAY11-7082 are specific inhibitors of PI3K p110α, PI3K p110β and NF-κB, respectively, and the concentrations used in the experiment were 32 nM, 5 nM and 10 μM, respectively. A total of 10 μl CCK-8 solution was added to each well. Subsequently, the cells were incubated for 2 h. A multimode plate reader (BioTek ELx808; BioTek Instruments, Inc.) was used to measure the absorbance at 450 nm.

Colony formation assay. ASPC-1/GEM cells were seeded into 6-well plates and subjected to various treatments for 24 h. Subsequently, the cells were trypsinized into single cells, seeded into 6-well plates (1,000 cells/well) and incubated at 37˚C with 5% carbon dioxide. After 14 days, the colonies were washed with PBS (Beyotime Institute of Biotechnology), fixed with 4% paraformaldehyde at room temperature for 30 min and stained with 0.1% crystal violet solution at room temperature for 10 min. The cells were washed thrice with double-distilled water. Images were captured with a digital camera after drying, and colonies containing >50 cells were counted.

Apoptosis assay. The cells were incubated in 6-well plates and subjected to various treatments. The cells were collected after 24 h, washed twice with cold PBS and resuspended in 500 μl cold binding buffer. Subsequently, 5 μl Annexin V-fluorescein isothiocyanate (BD Biosciences) was added. The mixture was protected from light and incubated at room temperature for 15 min. Finally, 5 μl propidium iodide was added 5 min prior to examination using a flow cytometer (BD Canto II; BD Biosciences).

Western blotting. Total, nuclear and membrane proteins were extracted separately using RIPA Lysis Buffer, the Nuclear and Cytoplasmic Protein Extraction Kit and the Membrane and Cytosol Protein Extraction Kit (Beyotime Institute of Biotechnology). The present study detected the expression levels of NF-κB in the nuclear protein samples, PI3K-p110α, PI3K-p110β and AKT in total protein samples, and P-gp, ABCG2 and MRP1 in membrane protein samples separately. Subsequently, the protein concentration was determined using a Bicinchoninic Acid Protein Assay kit (Beyotime Institute of Biotechnology). Protein was separated by 10 or 12% SDS-PAGE in four lanes and transferred to polyvinylidene

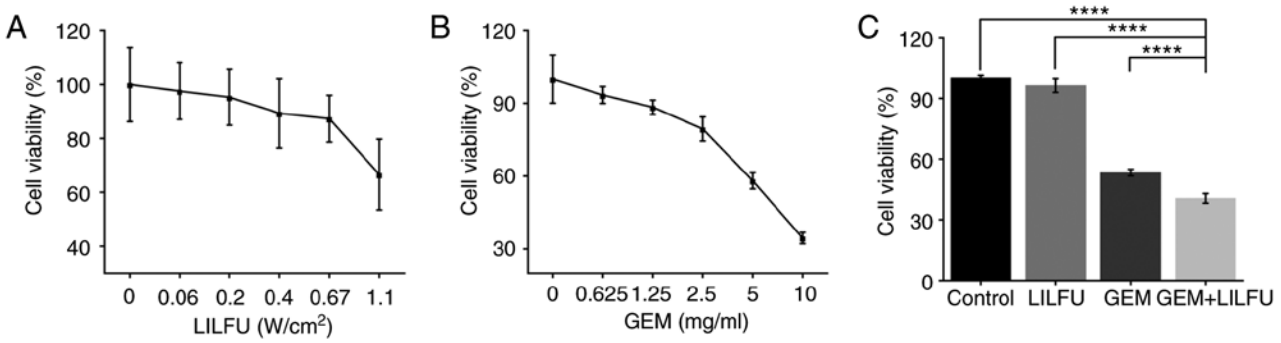

Figure 1. Viability of ASPC-1/GEM cells treated with LILFU and GEM. (A) Cell viability following exposure to LILFU with different acoustic intensities. (B) Cytotoxicity of GEM in ASPC-1/GEM cells. (C) ASPC-1/GEM cells treated with LILFU, GEM or GEM+LILFU. ****P<0.0001. ASPC-1/GEM cells, gemcitabine-resistant ASPC-1 cells; GEM, gemcitabine; LILFU, low-intensity low-frequency ultrasound.

difluoride membranes (EMD Millipore). The membranes were blocked with 5% skimmed milk at room temperature for 1 h, and incubated with primary antibodies overnight at 4˚C. Furthermore, the membranes were incubated with an appropriate horseradish peroxidase-conjugated secondary antibody (cat. no. 7074; dilution 1:1,000; Cell Signaling Technology, Inc.) at room temperature for 1 h. Finally, the target proteins were detected using enhanced chemiluminescence reagent (EMD Millipore). Enhanced chemiluminescence signals were examined and analyzed using Image Lab version 4.1 software (Bio-Rad Laboratories, Inc.). Antibodies against P-gp (cat. no. 13342; dilution 1:1,000), ABCG2 (cat. no. 42078; dilution 1:1,000), MRP1 (cat. no. 72202; dilution 1:1,000), PI3K-p110α (cat. no. 4249; dilution 1:1,000), PI3K-p110β (cat. no. 3011; dilution 1:1,000), AKT (cat. no. 4685; dilution 1:1,000), NF-κB (cat. no. 8242; dilution 1:1,000) and β-actin (cat. no. 4970; dilution 1:1,000) were purchased from Cell Signaling Technology, Inc.

Xenograft tumor model. A total of $1x10^7$ ASPC-1/GEM cells were subcutaneously inoculated into the right oxter of 6-week-old female BALB/c nude mice, weighing ~18-22 g (Shanghai SLAC Co.). A total of 20 mice were maintained. The environment of mice was at the SPF level. A cycle of 12 h of light and 12 h of dark were maintained each day. The temperature was ~25˚C and the humidity was around 50%. Mice were provided sufficient water and food. The bedding was changed twice a week. All feeding and operating procedures were approved by the Animal Ethics Committee of the Second Affiliated Hospital of Zhejiang University School of Medicine. Tumor volumes were calculated using the following formula: Volume (mm^3)=A (mm) x B $(mm)^2/2$, where A and B are the longest and shortest diameters, respectively. When the tumors grew to 50-100 mm^3, the mice were randomly divided into four groups: Control, LILFU, GEM and GEM+LILFU. The mice were anesthetized with pentobarbital (80 mg/kg) via intraperitoneal injection, and the experimental animals were fixed on the workbench. GEM was injected into the tail vein at a dose of 50 mg/kg (27-29). The ultrasonic transducer was fixed on the holder. The tumor surface was coated with medical ultrasonic couplant, and was placed directly under the transducer (Fig. S1). The parameters of the ultrasound were as follows: 360 kHz, 50% duty cycle (on 3 sec, off 3 sec), 5 min. Following treatment, whole blood samples were collected into prechilled heparinized tubes at t=5, 15, 30, 60, 120, 360 and 720 min and plasma was separated from whole blood. The mice were treated once every 3 days for a total of 15 days, and the experiment ended on day 21. We considered the average diameter of tumors to exceed 20 mm, tumor growth or metastasis rapidly to cause infection or necrosis, rapid weight loss of more than 15-20% as humane endpoints. Once the state of the mice reached the humane endpoints, the mice were immediately anesthetized with pentobarbital (80 mg/kg) and sacrificed by cervical dislocation. Each mouse only had a single subcutaneous tumor nodule. The GEM concentration in the plasma was measured by high-performance liquid chromatography (HPLC, AB Sciex Company). Fifty microliters of mouse plasma was mixed with 50 µl of methanol, and then GEM was extracted from the plasma by the addition of 3.5 ml of isopropanol/ethyl acetate (1:2.5, v/v). The samples were vortexed for 10 min and then centrifuged at 4,800 x g for 10 min. The supernatants were collected and evaporated to dryness under a gentle stream of nitrogen at 60˚C. The residue was dissolved in a 50 µl methanol and then centrifuged at 8,000 x g for 10 min before use. The flow rate of the mobile phase was 0.2 ml/min. Twenty microliters of sample was used to measure drug absorption at 268 nm. Standard curves for GEM were generated using commercially available compounds.

Immunohistochemical staining. Tumor specimens were fixed with 4% paraformaldehyde and embedded in paraffin. The slices were dewaxed, rehydrated, incubated with antigen retrieval solution (pH 6.0), processed with 30 ml/l hydrogen peroxide to block endogenous peroxidase activity and blocked with 4% normal goat serum (Beyotime Institute of Biotechnology). The slices were incubated with a mouse anti-human antibody against Ki-67 (cat. no. 9449, dilution 1:400, Cell Signaling Technology, Inc.) overnight at 4˚C, followed by incubation with a secondary anti-mouse biotin-conjugated antibody (cat. no. ab6788, dilution 1:1,000, Abcam) for 30 min at 37˚C. Subsequently, the slices were washed with PBS, developed using diaminobenzidine and counterstained with hematoxylin.

Statistical analysis. The normal distribution of experimental data was verified using the Shapiro-Wilk test. All data are presented as the mean ± standard deviation. Comparisons among multiple groups were performed using one-way

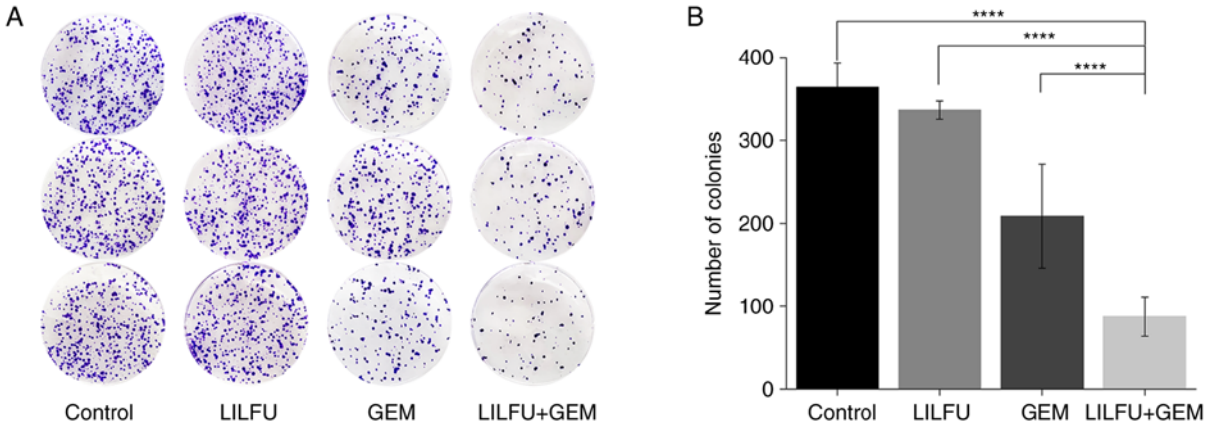

Figure 2. Effect of treatment with GEM+LILFU on the proliferation of ASPC-1/GEM cells. (A) Colony formation assay for cells treated with GEM, LILFU or GEM+LILFU for 2 weeks. The experiments were performed in triplicate. (B) Quantification of the colony formation assay. ****P<0.0001. ASPC-1/GEM cells, gemcitabine-resistant ASPC-1 cells; GEM, gemcitabine; LILFU, low-intensity low-frequency ultrasound.

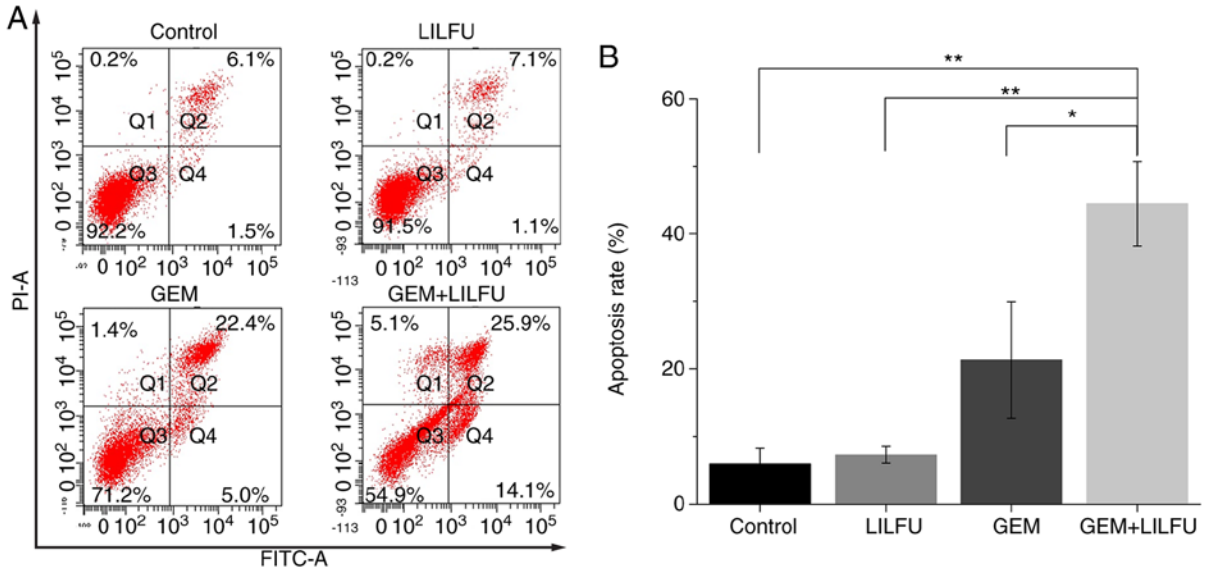

Figure 3. Effect of treatment with GEM+LILFU on apoptosis in ASPC-1/GEM cells. (A) ASPC-1/GEM cells were treated with GEM, LILFU or GEM+LILFU for 24 h, stained with Annexin V-FITC and PI, and examined using flow cytometry. (B) Quantification of apoptotic rates in the experiments. *P<0.05; **P<0.01. ASPC-1/GEM cells, gemcitabine-resistant ASPC-1 cells; FITC, fluorescein isothiocyanate; GEM, gemcitabine; LILFU, low-intensity low-frequency ultrasound; PI, propidium iodide.

ANOVA, and a post hoc test was performed using the Tukey's correction. P<0.05 was considered to indicate a statistically significant difference. All analyses were performed using SPSS Statistics version 20.0 software (IBM Corp.).

Results

Exposure to LILFU enhances GEM-induced cytotoxicity in ASPC-1/GEM cells. LILFU-irradiated cells were incubated for 24 h to identify the appropriate acoustic parameters which did not inhibit cell viability. Cell viability was >95% for an acoustic intensity of ≤0.2 W/cm^2 (Fig. 1A). Furthermore, the half-maximal inhibitory concentration of GEM was 6.63 mg/ml (Fig. 1B). The acoustic parameter of 0.2 W/cm^2 and the concentration of 6.63 mg/ml were used in the subsequent experiments. Furthermore, the cells were treated with GEM, LILFU or GEM+LILFU. The cell viability was 40.59% in the GEM+LILFU group compared with 53.29% in the GEM group, and the difference was statistically significant (Fig. 1C).

LILFU combined with GEM enhances the inhibition of ASPC-1/GEM cell proliferation. There was no apparent difference observed between the LILFU and control groups. The proliferative ability of the GEM group was lower than that observed in the control group, as demonstrated by the colony formation assay. The number of colonies was significantly reduced in the GEM+LILFU group compared with in the GEM group (88 vs. 209 colonies, respectively; Fig. 2A and B).

LILFU enhances GEM-induced apoptosis in ASPC-1/GEM cells. Flow cytometry was used to determine the apoptotic rates of the ASPC-1/GEM cells. The apoptotic rate of cells treated with GEM was 27.4%, which was higher than that

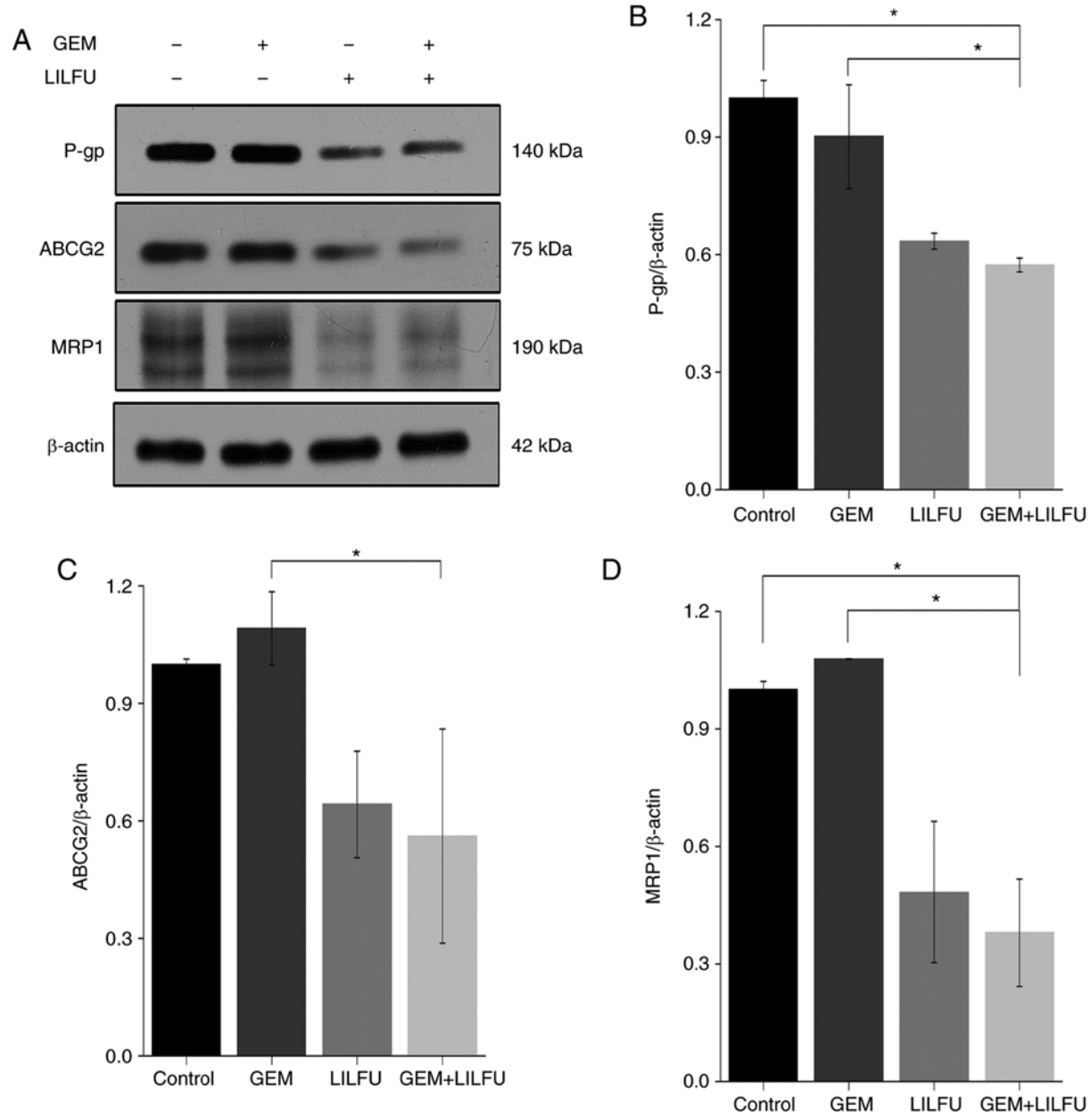

Figure 4. Expression levels of ABC transporters following treatment with GEM and LILFU. (A) Expression levels of P-gp, ABCG2 and MRP1 following treatment with GEM, LILFU or GEM+LILFU. (B-D) Semi-quantification of the expression levels of P-gp, ABCG2 and MRP1. *P<0.05. ABC, adenosine triphosphate-binding cassette; ABCG2, ABC subfamily G member 2; GEM, gemcitabine; LILFU, low-intensity low-frequency ultrasound; MRP1, multidrug resistance-associated protein 1; P-gp, P glycoprotein.

recorded in the control group. Furthermore, the apoptotic rate of cells treated with GEM+LILFU was 40%, which was significantly higher than that of cells treated with GEM (Fig. 3A and B).

Exposure to LILFU induces the reduction of ABC transporter expression. The present study revealed that the expression levels of P-gp, ABCG2 and MRP-1 were reduced in LILFU group compared to the Control group, whereas there was almost no change observed in the GEM group. Furthermore, the expression levels of P-gp, ABCG2 and MRP-1 were decreased more significantly in the GEM+LILFU group (Fig. 4A-D). This finding indicated that exposure to GEM+LILFU cause a reduction in the expression levels of these proteins.

Exposure to LILFU induces the reduction of PI3K/AKT/NF-κB pathway-associated protein expression. The expression levels of PI3K-p110α, PI3K-p110β, AKT and NF-κB were determined via western blotting to examine the effect of LILFU on the PI3K/AKT/NF-κB signaling pathway. The expression levels of PI3K-p110β and AKT were not markedly altered in the group, LILFU group or GEM+LILFU group compared to the control group (Fig. 5A, C and D). However, the expression levels of PI3K-p110α and NF-κB were decreased following treatment with GEM+LILFU compared with these levels in the GEM group (Fig. 5A, B and E).

In addition, ASPC-1/GEM cells were treated with GEM combined with A66 (PI3K-p110α inhibitor), TGX221 (PI3K-p110β inhibitor) and BAY11-7082 (NF-κB inhibitor).

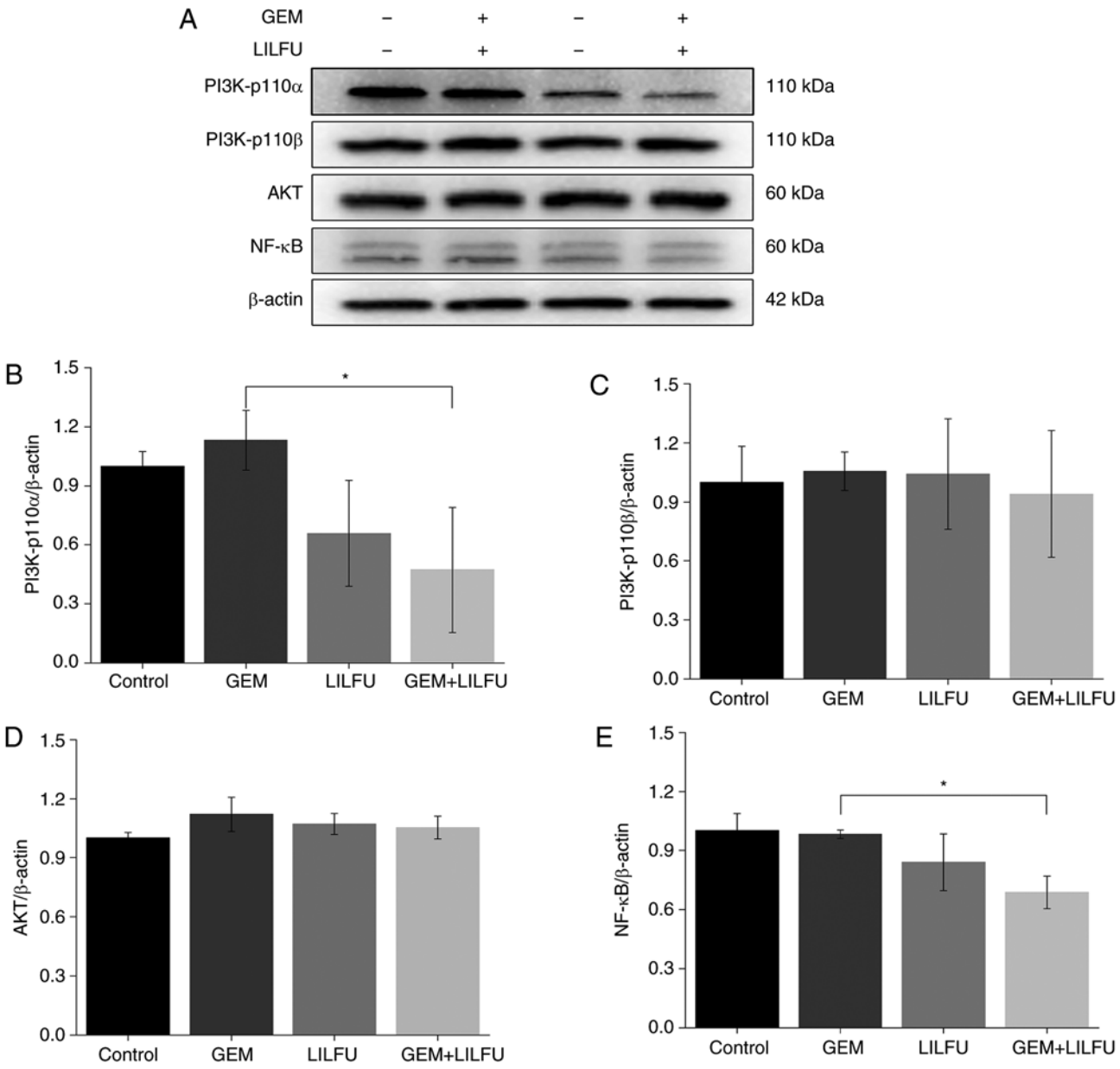

Figure 5. Expression levels of PI3K/AKT/NF-κB signaling pathway-associated proteins following treatment with GEM or LILFU. (A) Expression levels of PI3K-p110α, PI3K-p110β, AKT and NF-κB following treatment with GEM, LILFU or GEM+LILFU. (B-E) Semi-quantification of the expression levels. *P<0.05. GEM, gemcitabine; LILFU, low-intensity low-frequency ultrasound; PI3K, phosphoinositide 3-kinase; AKT, protein kinase B; NF-κB, nuclear factor-κB.

Firstly, the expression levels of PI3K-p110α, PI3K-p110β and NF-κB were determined. Subsequently, cell viability was detected using a CCK-8 assay. Following the combined treatments, the expression levels of PI3K-p110α, PI3K-p110β and NF-κB were reduced when compared to the GEM treated alone group (Fig. 6A-F). Cell viability was decreased in the GEM+A66 and GEM+BAY11-7082 groups when compared with the GEM alone treated group (Fig. 6G and I). However, the cell viability was not significantly decreased in the GEM+TGX221 group (Fig. 6H).

Exposure to LILFU enhances the effect of GEM in vivo. ASPC-1/GEM cell xenograft models were established to further identify the effect of LILFU *in vivo*. The blood concentration of GEM was 14.08 μg/ml at 5 min and then gradually decreased over time. (Fig. 7A). Tumors observed in the LULFU+GEM group were markedly smaller than those observed in the GEM group (Fig. 7B and C). Furthermore, immunohistochemical staining revealed that the expression level of Ki-67 was decreased in the GEM+LILFU group compared with that in the GEM group (Fig. 7D).

Discussion

Previous studies have identified various mechanisms of drug resistance in pancreatic ductal adenocarcinoma (PDAC). Firstly, ABC transporters are critical mediators of drug efflux, which leads to decreased intracellular accumulation of drugs and development of tumor drug resistance (TDR) (30,31). Secondly, critical genetic mutations contribute to TDR.

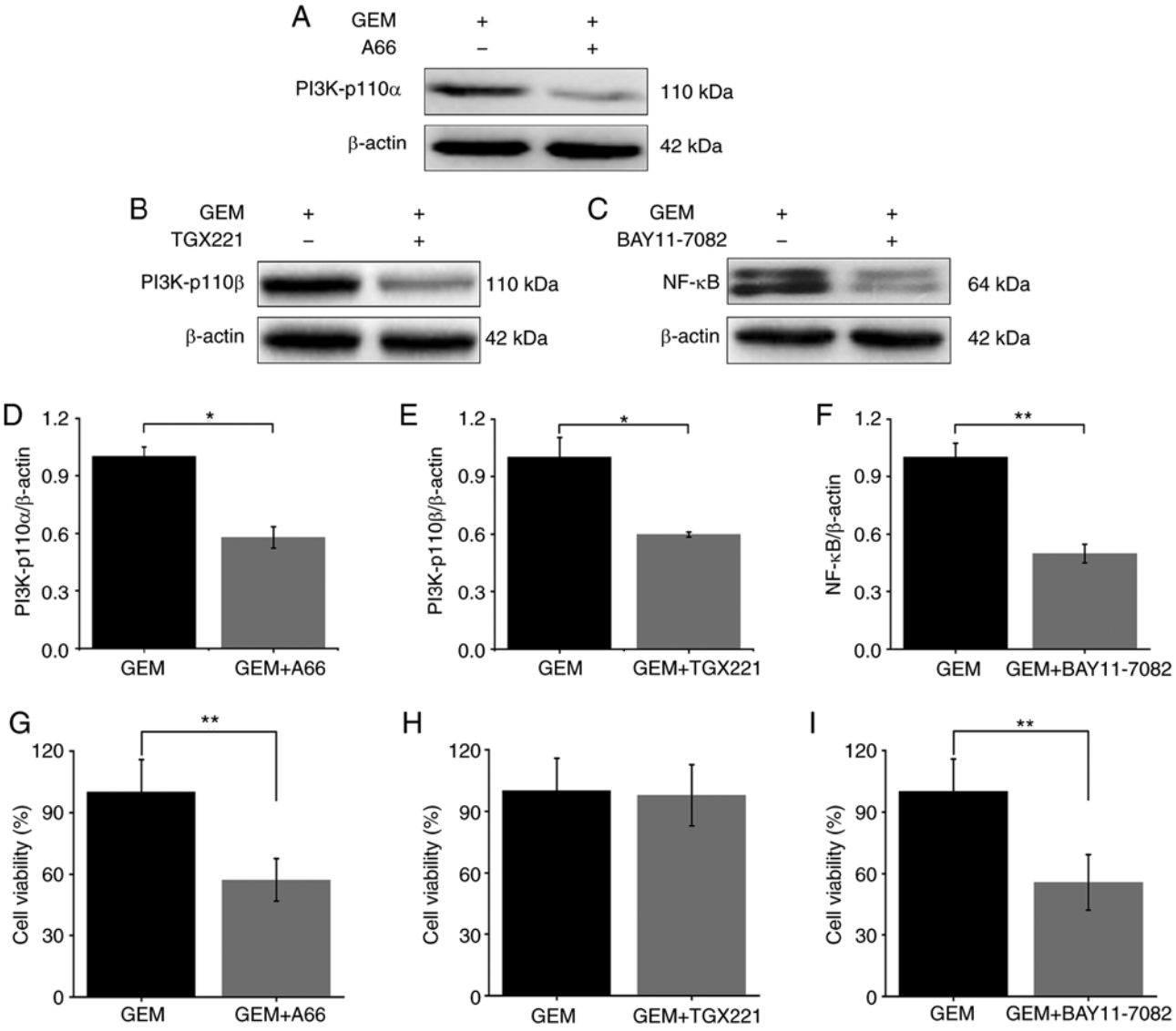

Figure 6. Protein expression and cell viability following PI3K/NF-κB inhibitor treatment. (A-F) Expression levels of PI3K-p110α, PI3K-p110β and NF-κB following treatment with A66, TGX221 and BAY11-7082. (G-I) Cell viability following treatment with A66, TGX221 and BAY11-7082. *P<0.05; **P<0.01. GEM, gemcitabine; PI3K, phosphoinositide 3-kinase; AKT, protein kinase B; NF-κB, nuclear factor-κB.

For example, tumors with the BRCA mutation exhibit increased resistance to carboplatin compared with tumors not harboring this mutation (32). Furthermore, numerous signaling pathways, including the PI3K/AKT/NF-κB and Notch signaling pathways, are involved in drug resistance in PDAC. Banerjee *et al*, demonstrated that activation of NF-κB is mostly associated with resistance to chemotherapy in PDAC (25).

Due to their short wavelength and high frequency, ultrasonic waves have strong directivity when propagating in the medium and strong penetrating power. At present, low-frequency ultrasound is used in various clinical fields, such as *in vivo* thrombolysis, analgesia, desensitization and dental surgery. Additionally, Yu *et al* reported that low-frequency ultrasound has a synergistic antibacterial effect on bacteria and chlamydia in combination with drugs or antibiotics (33). Therefore, ultrasound can serve a biological role under the premise of ensuring safety and feasibility within a certain frequency and intensity range.

Ultrasound can selectively increase the permeability of the tumor cell membrane to accumulate higher intracellular concentrations of drugs in the treatment of chronic myelogenous leukemia and ovarian carcinoma (34,35). Hassan *et al* (36) observed higher sensitivity in drug-resistant uterine sarcoma cells following exposure to ultrasound compared with in cells exhibiting a normal response to treatment. Therefore, ultrasound may improve the anticancer effect of doxorubicin in resistant cells (36). In addition, ultrasound-induced local hyperthermia was found to increase the cellular uptake of drugs and induce death of drug-resistant cells (37). Furthermore, Ning *et al* (38) reported that high-intensity focused ultrasound enhances the effect of bufalin by inducing apoptosis in PDAC. Liu *et al* chose ultrasound parameters with a frequency of 300 kHz, an average intensity of 1 W/cm^2, a time of 6 min, and a duty cycle of 50% to treat ovarian cancer xenografts *in vivo* (39). Huang *et al* chose ultrasound parameters with a frequency of 1 MHz, an average intensity of 0.74 W/cm^2, a time of 5 min, and a duty cycle of 20% both *in vitro* and *in vivo* (40). Wu *et al*

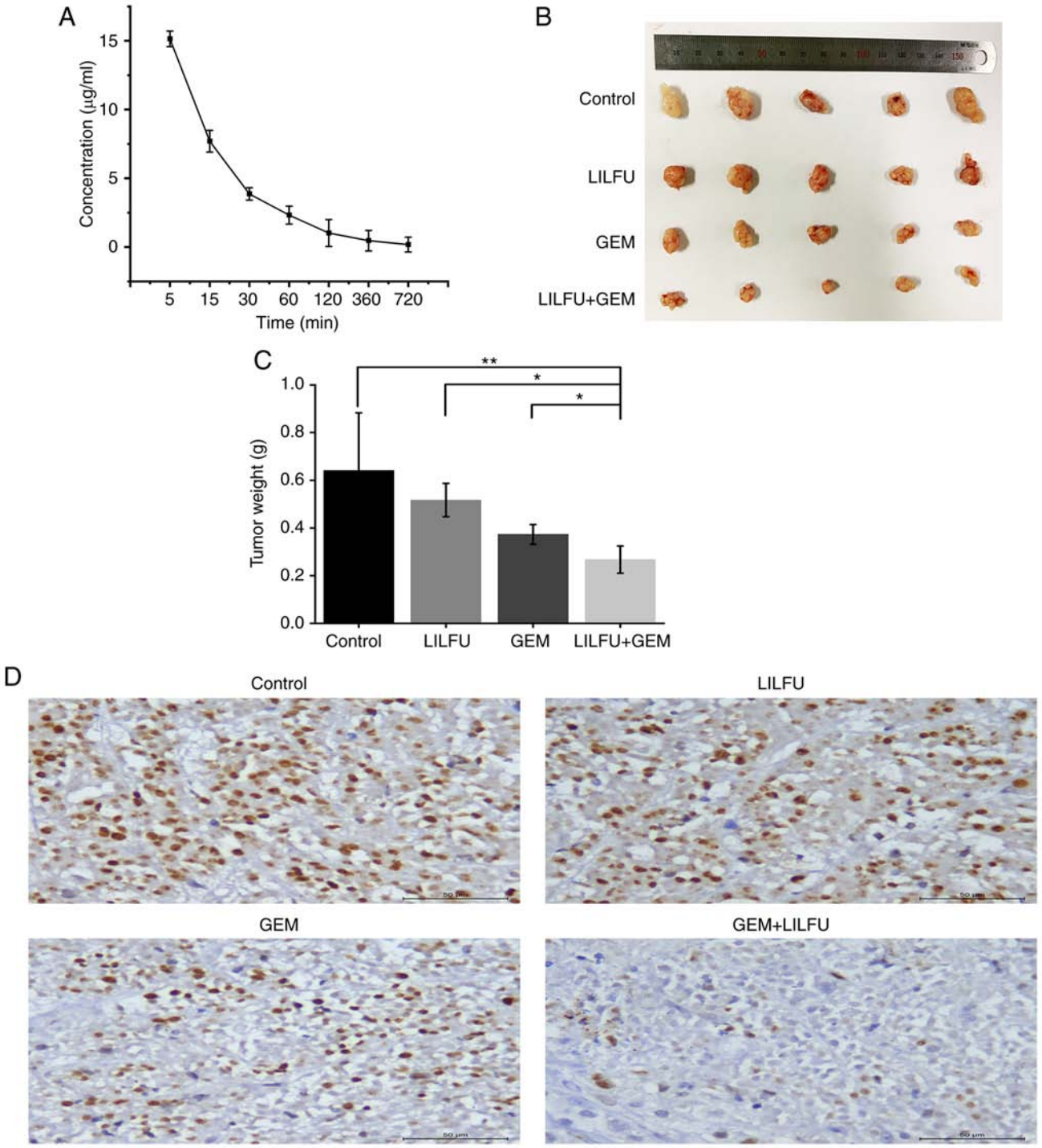

Figure 7. Exposure to LILFU enhances the effect of GEM *in vivo*. (A) The concentration of GEM after mice were treated. (B) Isolated tumors after treatment with LILFU, GEM or GEM+LILFU. (C) Quantitative analysis of tumor weight. (D) Expression levels of Ki-67. *P<0.05; **P<0.01. ASPC-1/GEM cells, gemcitabine-resistant ASPC-1 cells; GEM, gemcitabine; LILFU, low-intensity low-frequency ultrasound.

chose continuous ultrasound parameters with a frequency of 1 MHz, an average intensity of 1.2 W/cm^2, and a time of 10 sec (41). Hassan *et al* chose ultrasound parameters with a frequency of 1 MHz, an average intensity of 0.4 W/cm^2, a time of 1 min, and a duty cycle of 10% (36). Sun *et al* chose continuous ultrasound parameters with a frequency of 300 KHz, an average intensity of 1 W/cm^2, and a time of 40 sec (42). He *et al* chose ultrasound parameters with a frequency of 300 KHz, an average intensity of 2 W/cm^2, a time of 10 min both *in vitro* and *in vivo* (43). Liu *et al* chose ultrasound parameters with a frequency of 1 MHz, an average intensity of 0.4 W/cm^2, a time of 20 min (37). Based on the above references and our previous experiments, we chose ultrasound parameters with a frequency of 360 KHz, an average intensity of 0.2 W/cm^2, a time of 5 min, and a duty cycle of 50% *in vivo*.

Based on the characteristics of ultrasound, the present study aimed to use LILFU to reverse TDR in PDAC. The present study demonstrated that LILFU enhanced the effect of GEM, and suggested a possible underlying mechanism by which LILFU reversed TDR. Overexpression of the ABC transporters, which

pump chemotherapeutic drugs out of the cytoplasm, invariably leads to the development of TDR. The expression levels of P-gp are low prior to treatment. However, the expression levels are upregulated after chemotherapy which contributes to TDR (44). In the present study, inhibition of ABC transporter expression by LILFU, accompanied by the administration of intracellular chemotherapeutic drugs, markedly increased the antitumor efficacy of the agents. Following exposure to LILFU, the expression levels of P-gp, ABCG2 and MRP1 were decreased, suggesting that LILFU reversed TDR via ABC transporters. Furthermore, LILFU has some advantages over traditional inhibitors of ABC transporters. Firstly, LILFU is more accurate than chemical inhibitors and can target tumor lesions, potentially preventing the development of systemic side effects caused by treatment. In addition, similar to light beam treatment, LILFU is a type of easily assessable physical energy, which can be applied *in vivo* through a non-invasive approach without decreasing the penetration ability.

Previous studies have demonstrated that the PI3K/AKT signaling pathway is a mediator of chemoresistance in PDAC (45,46). Zhang *et al* (47), demonstrated that overexpression of galectin-1 activates the PI3K/AKT signaling pathway, and PI3K/AKT cascade activation induces hepatocellular carcinoma resistance to sorafenib and promotes the progression of liver cancer. Furthermore, Liang *et al* (48) reported that STAT3 phosphorylation activates the PI3K/AKT signaling pathway, which leads to increased cisplatin resistance in ovarian cancer. To *et al* (49), demonstrated that CUDC-907 is a *PI3K* inhibitor and exhibits a synergistic cytotoxic effect on cisplatin-resistant cancer cells in combination therapy with cisplatin. Furthermore, CUDC-907 was found to reverse cancer cell resistance by inhibiting ABCC2 which is one of the ABC transporters.

Examination of the ubiquitously expressed PI3K-p110 has revealed the distinct and various roles of each subunit in the cell. However, in previous studies, it has been unclear whether PI3K-p110α or PI3K-p110β is involved in the reversion of TDR. Furthermore, previous studies have rarely investigated the effect of ultrasound treatment on the PI3K/AKT/NF-κB signaling pathway. In the present study, the expression levels of PI3K-p110α were decreased following GEM+LILFU treatment, whereas the expression levels of PI3K-p110β were not significantly altered. Therefore, it was concluded that PI3K-p110α, rather than PI3K-p110β, may be involved in TDR. In future studies, PI3K-p110α may be a target of the PI3K signaling pathway and can be inhibited to reverse TDR. Ma *et al* (50), treated pancreatic cancer with triptolide and GEM, revealing that triptolide enhances the sensitivity of pancreatic cancer cells to GEM by inhibiting NF-κB signaling. Furthermore, the involvement of NF-κB in the PI3K/AKT signaling pathway is commonly ignored. Therefore, its role in TDR may have been overlooked. Additionally, NF-κB expression is markedly reduced following GEM+LILFU treatment, suggesting that it may also serve an essential role in LILFU-induced reversion of TDR. As is known to us, NF-κB is bound and inhibited by Inhibitor κB (IκB) proteins in cytoplasm and is kept in an inactive state (51). IKKα activated by the PI3K/AKT signaling pathway phosphorylates IκB proteins and then IκB proteins are exposed to proteasomal degradation, resulting in nuclear translocation and transcriptional activation of NF-κB (52). We propose the hypothesis that LILFU inhibited the PI3K-p110α/AKT signaling pathway, causing IKKα to be inactive, thus preventing IκB from being phosphorylated. Thus, IκB still bound to NF-κB and inhibited NF-κB activation and nuclear translocation, which caused the reduction of NF-κB in the nucleus. In addition, the present study inhibited PI3K-p110β using TGX221, and the cell viability in the TGX221 group was not significantly altered compared with GEM group. However, when PI3K-p110α and NF-κB were inhibited, the cell viability in the A66 and BAY11-7082 groups were markedly decreased. Therefore, LILFU may enhance chemosensitivity via the PI3K-p110α/AKT/NF-κB signaling pathway.

Hien *et al* (53) revealed that puerarin reduced the expression levels of P-gp via the NF-κB signaling pathway in breast cancer, which was consistent with the downregulation of NF-κB observed in the present study. Previous studies have revealed that the PI3K inhibitor CUDC-907 reverses the resistance of cancer cells by inhibiting ABCC2 which is one of the ABC transporters (49). Therefore, it was concluded that LILFU may downregulate the expression levels of ABC transporters (P-gp, ABCG2 and MRP1) by inhibiting the PI3K-p110α/AKT/NF-κB signaling pathway, thereby reversing the resistance of pancreatic cancer.

LILFU has some obvious advantages over inhibitors of ABC transporters and the PI3K/AKT/NF-κB signaling pathway. Firstly, compared with chemical inhibitors, LILFU is more accurate and can accumulate in tumor tissues without causing systemic side effects. In addition, LILFU is more penetrating and can affect the deep parts of organs or tissues. Therefore, LILFU can produce biological effects in the body.

The present study used LILFU to reverse TDR without apparent side effects. Combination treatment of chemotherapeutic agents and LILFU may improve the chemosensitivity of cancer. Therefore, LILFU may be a novel, non-invasive and promising strategy for the reversion of TDR. Importantly, the combination treatment considerably decreased the tumor volume in a xenograft mouse model. This finding demonstrated that the LILFU-induced increase in chemosensitivity *in vivo* is feasible, effective and safe. In future studies, the LILFU intensity treatment window or threshold should be explored to determine the treatment parameters more precisely. Furthermore, the association between ABC transporters and the PI3K/AKT/NF-κB signaling pathway in TDR should be elucidated, with the aim to further reverse TDR.

In conclusion, LILFU improved the chemosensitivity of ASPC-1/GEM cells, inhibited cell viability and proliferation, and promoted cell apoptosis in the GEM+LILFU group. LILFU reversed TDR by inhibiting the expression of ABC transporters, including P-gp, ABCG2 and MRP-1. Furthermore, LILFU may reverse TDR by inhibiting PI3K-p110α and NF-κB, instead of PI3K-p110β, in the PI3K/AKT/NF-κB signaling pathway. Therefore, it was concluded that LILFU may downregulate the expression levels of ABC transporters, including P-gp, ABCG2 and MRP1, by inhibiting the PI3K-p110α/AKT/NF-κB signaling pathway, thereby reversing resistance in pancreatic cancer. Furthermore, treatment with GEM+LILFU inhibited the growth of xenograft tumors *in vivo* more effectively compared with GEM alone, and decreased the protein expression levels of Ki-67. Moreover, several groups could be added for mice inoculated with cells pretreated by GEM with or without LILFU before surgery, which was a limitation of our study, to more fully illustrate the effect of GEM+LILFU.

The results of the present study revealed that LILFU is a promising treatment option for the reversal of TDR. Further clinical studies are required to assess the feasibility and efficacy of LILFU in reversing TDR.

Acknowledgements

The GEM-resistant ASPC-1 (ASPC-1/GEM) cell line was provided by Professor Min Li (University of Oklahoma, Norman, OK, USA).

Funding

The present study was supported by the National Natural Science Foundation of China (grant nos. 81527803 and 81420108018), National Key R&D Program of China (grant no. 2018YFC0115900), Zhejiang Science and Technology Project (grant no. 2019C03077), Youth Natural Science Fund Project of Zhejiang Province (grant no. LQ19H180004), and Natural Science Fund Project of Ningbo (grant no. 2018A610380).

Availability of data and materials

All data generated or analyzed during this study are included in this published article.

Authors' contributions

FQ performed the majority of the experiments and wrote the article. JCh performed the majority of the analysis of data and helped write the article. JCa and FD assisted with the experiments. PH was in charge of project design and writing of the article. All authors read and approved the manuscript and agree to be accountable for all aspects of the research in ensuring that the accuracy or integrity of any part of the work are appropriately investigated and resolved.

Ethics approval and consent to participate

The experimentation using nude mice was approved by the Animal Ethics Committee of the Second Affiliated Hospital of Zhejiang University School of Medicine.

Patient consent for publication

Not applicable.

Competing interests

The authors declare that they have no competing interests.

References

1. Bray F, Ferlay J, Soerjomataram I, Siegel RL, Torre LA and Jemal A: Global cancer statistics 2018: GLOBOCAN estimates of incidence and mortality worldwide for 36 cancers in 185 countries. CA Cancer J Clin 68: 394-424, 2018.
2. Kamisawa T, Wood LD, Itoi T and Takaori K: Pancreatic cancer. Lancet 388: 73-85, 2016.
3. Siegel RL, Miller KD and Jemal A: Cancer statistics, 2018. CA Cancer J Clin 68: 7-30, 2018.
4. Saad AM, Turk T, Al-Husseini MJ and Abdel-Rahman O: Trends in pancreatic adenocarcinoma incidence and mortality in the United States in the last four decades; a SEER-based study. BMC Cancer 18: 688, 2018.
5. de Sousa Cavalcante L and Monteiro G: Gemcitabine: Metabolism and molecular mechanisms of action, sensitivity and chemoresistance in pancreatic cancer. Eur J Pharmacol 741: 8-16, 2014.
6. Ina S, Hirono S, Noda T and Yamaue H: Identifying molecular markers for chemosensitivity to gemcitabine in pancreatic cancer: Increased expression of interferon-stimulated gene 15 kd is associated with intrinsic chemoresistance. Pancreas 39: 473-485, 2010.
7. Luo W, Yang G, Qiu J, Luan J, Zhang Y, You L, Feng M, Zhao F, Liu Y, Cao Z, *et al*: Novel discoveries targeting gemcitabine-based chemoresistance and new therapies in pancreatic cancer: How far are we from the destination? Cancer Med 8: 6403-6413, 2019.
8. Chiorean EG, Cheung WY, Giordano G, Kim G and Al-Batran SE: Real-world comparative effectiveness of nab-paclitaxel plus gemcitabine versus FOLFIRINOX in advanced pancreatic cancer: A systematic review. Ther Adv Med Oncol 11: 1758835919850367, 2019.
9. Vasan N, Baselga J and Hyman DM: A view on drug resistance in cancer. Nature 575: 299-309, 2019.
10. Aleksakhina SN, Kashyap A and Imyanitov EN: Mechanisms of acquired tumor drug resistance. Biochim Biophys Acta Rev Cancer 1872: 188310, 2019.
11. Mohammad IS, He W and Yin L: Understanding of human ATP binding cassette superfamily and novel multidrug resistance modulators to overcome MDR. Biomed Pharmacother 100: 335-348, 2018.
12. Lowrence RC, Subramaniapillai SG, Ulaganathan V and Nagarajan S: Tackling drug resistance with efflux pump inhibitors: From bacteria to cancerous cells. Crit Rev Microbiol 45: 334-353, 2019.
13. Bugde P, Biswas R, Merien F, Lu J, Liu DX, Chen M, Zhou S and Li Y: The therapeutic potential of targeting ABC transporters to combat multi-drug resistance. Expert Opin Ther Targets 21: 511-530, 2017.
14. Fletcher JI, Williams RT, Henderson MJ, Norris MD and Haber M: ABC transporters as mediators of drug resistance and contributors to cancer cell biology. Drug Resist Updat 26: 1-9, 2016.
15. Adamska A and Falasca M: ATP-binding cassette transporters in progression and clinical outcome of pancreatic cancer: What is the way forward? World J Gastroenterol 24: 3222-3238, 2018.
16. Falasca M and Linton KJ: Investigational ABC transporter inhibitors. Expert Opin Investig Drugs 21: 657-666, 2012.
17. Cui H, Zhang AJ, Chen M and Liu JJ: ABC Transporter inhibitors in reversing multidrug resistance to chemotherapy. Curr Drug Targets 16: 1356-1371, 2015.
18. Bates S, Kang M, Meadows B, Bakke S, Choyke P, Merino M, Goldspiel B, Chico I, Smith T, Chen C, *et al*: A Phase I study of infusional vinblastine in combination with the P-glycoprotein antagonist PSC 833 (valspodar). Cancer 92: 1577-1590, 2001.
19. Knuefermann C, Lu Y, Liu B, Jin W, Liang K, Wu L, Schmidt M, Mills GB, Mendelsohn J and Fan Z: HER2/PI-3K/Akt activation leads to a multidrug resistance in human breast adenocarcinoma cells. Oncogene 22: 3205-3212, 2003.
20. Wang W, Xiao Y, Li S, Zhu X, Meng L, Song C, Yu C, Jiang N and Liu Y: Synergistic activity of magnolin combined with B-RAF inhibitor SB590885 in hepatocellular carcinoma cells via targeting PI3K-AKT/mTOR and ERK MAPK pathway. Am J Transl Res 11: 3816-3824, 2019.
21. Gao X, Qin T, Mao J, Zhang J, Fan S, Lu Y, Sun Z, Zhang Q, Song B and Li L: PTENP1/miR-20a/PTEN axis contributes to breast cancer progression by regulating PTEN via PI3K/AKT pathway. J Exp Clin Cancer Res 38: 256, 2019.
22. Maira SM, Pecchi S, Huang A, Burger M, Knapp M, Sterker D, Schnell C, Guthy D, Nagel T, Wiesmann M, *et al*: Identification and characterization of NVP-BKM120, an orally available pan-class I PI3-kinase inhibitor. Mol Cancer Ther 11: 317-328, 2012.
23. Hirai H, Sootome H, Nakatsuru Y, Miyama K, Taguchi S, Tsujioka K, Ueno Y, Hatch H, Majumder PK, Pan BS and Kotani H: MK-2206, an allosteric Akt inhibitor, enhances antitumor efficacy by standard chemotherapeutic agents or molecular targeted drugs in vitro and in vivo. Mol Cancer Ther 9: 1956-1967, 2010.
24. Ghobrial IM, Witzig TE and Adjei AA: Targeting apoptosis pathways in cancer therapy. CA Cancer J Clin 55: 178-194, 2005.

25. Banerjee S, Wang Z, Kong D and Sarkar FH: 3,3'-Diindolylmethane enhances chemosensitivity of multiple chemotherapeutic agents in pancreatic cancer. Cancer Res 69: 5592-5600, 2009.
26. Bharti AC and Aggarwal BB: Nuclear factor-kappa B and cancer: Its role in prevention and therapy. Biochem Pharmacol 64: 883-888, 2002.
27. Ng SS, Tsao MS, Nicklee T and Hedley DW: Wortmannin inhibits pkb/akt phosphorylation and promotes gemcitabine antitumor activity in orthotopic human pancreatic cancer xenografts in immunodeficient mice. Clin Cancer Res 7: 3269-3275, 2001.
28. Gilles ME, Maione F, Cossutta M, Carpentier G, Caruana L, Di Maria S, Houppe C, Destouches D, Shchors K, Prochasson C, *et al*: Nucleolin targeting impairs the progression of pancreatic cancer and promotes the normalization of tumor vasculature. Cancer Res 76: 7181-7193, 2016.
29. Yoon Y, Lim JW, Kim J, Kim Y and Chun KH: Discovery of ursolic acid prodrug (NX-201): Pharmacokinetics and in vivo antitumor effects in PANC-1 pancreatic cancer. Bioorg Med Chem Lett 26: 5524-5527, 2016.
30. Gottesman MM and Ambudkar SV: Overview: ABC transporters and human disease. J Bioenerg Biomembr 33: 453-458, 2001.
31. Lage H: An overview of cancer multidrug resistance: A still unsolved problem. Cell Mol Life Sci 65: 3145-3167, 2008.
32. Tutt AN, Lord CJ, McCabe N, Farmer H, Turner N, Martin NM, Jackson SP, Smith GC and Ashworth A: Exploiting the DNA repair defect in BRCA mutant cells in the design of new therapeutic strategies for cancer. Cold Spring Harb Symp Quant Biol 70: 139-148, 2005.
33. Yu H, Chen S and Cao P: Synergistic bactericidal effects and mechanisms of low intensity ultrasound and antibiotics against bacteria: A review. Ultrason Sonochem 19: 377-382, 2012.
34. Yu T, Hu K, Bai J and Wang Z: Reversal of adriamycin resistance in ovarian carcinoma cell line by combination of verapamil and low-level ultrasound. Ultrason Sonochem 10: 37-40, 2003.
35. Yang S, Wang P, Wang X, Su X and Liu Q: Activation of microbubbles by low-level therapeutic ultrasound enhances the antitumor effects of doxorubicin. Eur Radiol 24: 2739-2753, 2014.
36. Hassan MA, Furusawa Y, Minemura M, Rapoport N, Sugiyama T and Kondo T: Ultrasound-induced new cellular mechanism involved in drug resistance. PLoS One 7: e48291, 2012.
37. Liu Y, Cho CW, Yan X, Henthorn TK, Lillehei KO, Cobb WN and Ng KY: Ultrasound-Induced hyperthermia increases cellular uptake and cytotoxicity of P-glycoprotein substrates in multi-drug resistant cells. Pharm Res 18: 1255-1261, 2001.
38. Ning Z, Zhu Z, Wang H, Zhang C, Xu L, Zhuang L, Yan X, Wang D, Wang P and Meng Z: High-intensity focused ultrasound enhances the effect of bufalin by inducing apoptosis in pancreatic cancer cells. OncoTargets Ther 12: 1161-1170, 2019.
39. Liu L, Chang S, Sun J, Zhu S, Yin M, Zhu Y, Wang Z and Xu RX: Ultrasound-mediated destruction of paclitaxel and oxygen loaded lipid microbubbles for combination therapy in ovarian cancer xenografts. Cancer Lett 361: 147-154, 2015.
40. Huang C, Huang S, Li H, Li X, Li B, Zhong L, Wang J, Zou M, He X, Zheng H, *et al*: The effects of ultrasound exposure on P-glycoprotein-mediated multidrug resistance in vitro and in vivo. J Exp Clin Cancer Res 37: 232, 2018.
41. Wu Y, Liu X, Qin Z, Hu L and Wang X: Low-frequency ultrasound enhances chemotherapy sensitivity and induces autophagy in PTX-resistant PC-3 cells via the endoplasmic reticulum stress-mediated PI3K/Akt/mTOR signaling pathway. OncoTargets Ther 11: 5621-5630, 2018.
42. Sun Y, Li Q, Xu Y, Pu C, Zhao L, Guo Z, Ding X and Jin X: Study of the mechanisms underlying the reversal of multidrug resistance of human neuroblastoma multidrug-resistant cell line SK-N-SH/MDR1 by low-intensity pulsed ultrasound. Oncol Rep 29: 1939-1945, 2013.
43. He Y, Bi Y, Ji XJ and Wei G: Increased efficiency of testicular tumor chemotherapy by ultrasound microbubble-mediated targeted transfection of siMDR1. Oncol Rep 34: 2311-2318, 2015.
44. Nieth C and Lage H: Induction of the ABC-transporters Mdr1/P-gp (Abcb1), mrpl (Abcc1), and bcrp (Abcg2) during establishment of multidrug resistance following exposure to mitoxantrone. J Chemother 17: 215-223, 2005.
45. Kim MP and Gallick GE: Gemcitabine resistance in pancreatic cancer: Picking the key players. Clin Cancer Res 14: 1284-1285, 2008.
46. Andersson R, Aho U, Nilsson BI, Peters GJ, Pastor-Anglada M, Rasch W and Sandvold ML: Gemcitabine chemoresistance in pancreatic cancer: Molecular mechanisms and potential solutions. Scand J Gastroenterol 44: 782-786, 2009.
47. Zhang PF, Li KS, Shen YH, Gao PT, Dong ZR, Cai JB, Zhang C, Huang XY, Tian MX, Hu ZQ, *et al*: Galectin-1 induces hepatocellular carcinoma EMT and sorafenib resistance by activating FAK/PI3K/AKT signaling. Cell Death Dis 7: e2201, 2016.
48. Liang F, Ren C, Wang J, Wang S, Yang L, Han X, Chen Y, Tong G and Yang G: The crosstalk between STAT3 and p53/RAS signaling controls cancer cell metastasis and cisplatin resistance via the Slug/MAPK/PI3K/AKT-mediated regulation of EMT and autophagy. Oncogenesis 8: 59, 2019.
49. To KK and Fu LW: CUDC-907, a dual HDAC and PI3K inhibitor, reverses platinum drug resistance. Invest New Drugs 36: 10-19, 2018.
50. Ma JX, Sun YL, Yu Y, Zhang J, Wu HY and Yu XF: Triptolide enhances the sensitivity of pancreatic cancer PANC-1 cells to gemcitabine by inhibiting TLR4/NF-κB signaling. Am J Transl Res 11: 3750-3760, 2019.
51. Mulero MC, Wang VY, Huxford T and Ghosh G: Genome reading by the NF-κB transcription factors. Nucleic Acids Res 47: 9967-9989, 2019.
52. Solt LA and May MJ: The IkappaB kinase complex: Master regulator of NF-kappaB signaling. Immunol Res 42: 3-18, 2008.
53. Hien TT, Kim HG, Han EH, Kang KW and Jeong HG: Molecular mechanism of suppression of MDR1 by puerarin from Pueraria lobata via NF-kappaB pathway and cAMP-responsive element transcriptional activity-dependent up-regulation of AMP-activated protein kinase in breast cancer MCF-7/adr cells. Mol Nutr Food Res 54: 918-928, 2010.